Catalysis Today 227 (2014) 171–178

Contents lists available at ScienceDirect

Catalysis Today

journal homepage: www.elsevier.com/locate/cattod

Tuning the acidic and textural properties of ordered mesoporous silicas for their application as catalysts in the etherification of glycerol with isobutene

María Dolores González[a], Pilar Salagre[a], Robert Mokaya[b], Yolanda Cesteros[a,*]

[a] Departament de Química Física i Inorgànica, Universitat Rovira i Virgili, C/Marcel·lí Domingo s/n, 43007 Tarragona, Spain
[b] School of Chemistry, University of Nottingham, University Park, Nottingham NG7 2RD, UK

ARTICLE INFO

Article history:
Received 30 June 2013
Received in revised form 8 October 2013
Accepted 11 October 2013
Available online 9 November 2013

Keywords:
Glycerol etherification
Acid-functionalization
MCM-41
SBA-15
HMS
Textural porosity

ABSTRACT

Several silicas (MCM-41, SBA-15 and HMS) were acid-modified by incorporating aluminium or by introducing phosphorus species or sulfonic groups. The modified silicas maintained mesostructural ordering and a narrow pore size distribution. However, Their surface area and pore volume was lower than that of unmodified samples. The incorporation of aluminum in the structure of MCM-41 and SBA-15 increased the amount of Brønsted acid sites, leading to greater catalytic activity (i.e., higher conversion values) for glycerol etherification with isobutene than pure silicas, but their relatively weak acid strength resulted in low selectivity to di- and tri-tertiary butyl ethers of glycerol (h-GTBE). The introduction of phosphoric groups, with higher acidity strength, improved the selectivity to h-GTBE, and glycerol triether was detected in low amounts. Interestingly, HMS synthesized with dodecylamine and later sulfonated exhibited total conversion and 84% of selectivity to h-GTBE (26% to glycerol triether) after 24 h of reaction. The presence of textural mesoporosity in HMS reduced diffusion limitations, and consequently increased the incorporation of sulfonic groups and their accessibility, leading to higher catalytic activity.

1. Introduction

In the last few years, the catalytic etherification of glycerol (glycerine or 1,2,3-propanetriol), in the presence of *tert*-butanol or isobutene, to obtain di- and tri- tertiary butyl ethers of glycerol (h-GTBE) has been extensively studied [1–19]. h-GTBE can be used as oxygenated fuel in place of the environmentally highly toxic methyl tertiary butyl ether (MTBE), and to remarkably reduce emissions of particulate matter [20]. Additionally, this reaction is a challenging option for glycerol revalorization.

To date, the best catalytic results for etherification of glycerol have been achieved with strong acid ion exchange resins (Amberlyst type) as catalysts [1–4]. The incorporation of organosulfonic acid groups in mesoporous materials can generate effective solid acid catalysts with enhanced catalytic properties. Mesoporous silica SBA-15 functionalized with organosulfonic acid groups, introduced by conventional heating, resulted in high conversion and moderate selectivity values to h-GTBE for glycerol etherification with isobutene [5,6]. In a previous study, we prepared an organosulfonic acid functionalized SBA-15 by direct synthesis in one step microwave process. The resulting catalyst achieved total conversion and 91% to selectivity to h-GTBE (with 36% of selectivity to the glycerol triether) after 4 h of reaction for the etherification of glycerol with isobutene [16]. Apart from these studies of organosulfonic acid-functionalized SBA-15, there are no reports on the use of other mesoporous silicas such as MCM-41 or HMS modified by incorporation of Al, phosphorus species or sulfonic groups, as catalysts for glycerol etherification.

The incorporation of Al into the walls of MCM-41 or SBA-15 can generate active sites for adsorption, ion exchange and catalysis, which may function in aqueous media in a manner similar to that of aluminosilicate zeolites [21,22]. Zeolites are extensively used as acid catalysts, adsorbents and ion exchangers but their microporosity limits their applications to small molecules, and processes involving larger organic or biological molecules are excluded. Mesoporous molecular sieves have attracted much interest because of their potential application in reactions or separations involving bulky molecules. Aluminium is usually introduced into MCM-41 and SBA-15 by direct synthesis [23,24] or by post-synthesis grafting methods [25,26].

Another alternative to improve acidity in mesoporous materials and zeolites is to introduce phosphorus species. Kawi and co-workers proposed incorporation of phosphorous moieties onto MCM-41 via impregnation in H_3PO_4 solution [27]. More recently,

* Corresponding author. Tel.: +34 977558785; fax: +34 977559563.
E-mail address: yolanda.cesteros@urv.cat (Y. Cesteros).

0920-5861/$ – see front matter © 2013 Elsevier B.V. All rights reserved.
http://dx.doi.org/10.1016/j.cattod.2013.10.029

McKeen and co-workers incorporated organic sulfonic, carboxylic and phosphoric acid groups into zeolite Beta, MCM-41 and MCM-48 [28] and observed that the order of proton conductivities in the functionalized materials was sulfonic acid groups > phosphoric acid groups > carboxylic acid groups.

HMS is a hexagonal mesoporous silica which shows significant differences compared to MCM-41 in that it exhibits complementary extra-framework (i.e., textural) mesopores in addition to framework pores. Textural mesopores are important because they greatly facilitate mass transport to the framework. For this reason the catalytic reactivity of HMS is usually superior to MCM-41, especially for reactions involving large substrates in a liquid reaction medium where the reaction rates are limited by diffusion [29,30]. It is now known that the degree of textural mesoporosity is quite sensitive to both the solvent and the nature of the surfactant used in the synthesis of HMS [31].

The aim of this work was to generate several mesoporous silicas with varying amount and strength of Brønsted acid sites and test their catalytic activity for glycerol etherification with isobutene. The acidic properties of the mesoporous silicas were varied via a number of routes, namely; (a) incorporation of aluminium via post-synthesis alumination of MCM-41 and SBA-15, (b) introduction of phosphorus species in MCM-41 and SBA-15, (c) sulfonation of MCM-41 via direct synthesis, and (d) post-synthesis sulfonation of several HMS samples synthesized with surfactants of varying length.

2. Experimental

2.1. Catalyst preparation

2.1.1. Synthesis of mesoporous silicas: MCM-41 and SBA-15

MCM-41: Tetramethylammonium hydroxide (TMAOH) and cetyltrimethylammonium bromide (CTAB) were dissolved in distilled water by stirring at 308 K to generate a template solution. Fumed silica was added to the template solution under stirring for 1 h to have a molar composition of 1 Si:0.25 CTAB:0.2 TMAOH:40 H_2O. After further stirring for 1 h the resulting gel was aged at room temperature for 20 h and then transferred to a Teflon-lined autoclave and heated at 423 K for 48 h. The solid was recovered by filtration, washed, dried in air at room temperature, and calcined at 823 K for 8 h.

SBA-15: An amount of 4.0 g triblock copolymer poly(ethylene glycol)-block-poly(propylene glycol)-block-poly(ethylene glycol) ($EO_{20}PO_{20}EO_{20}$) was added to a solution of 25 g HCl (35% wt%) and 125 g water under stirring. After stirring for 2 h, the copolymer was completely dissolved after which 8.6 g tetraethyl orthosilicate (TEOS) was added. Following continuous stirring at 313 K for 20 h, the reaction mixture was transferred to a Teflon-lined autoclave and heated at 373 K for 24 h. The resulting product was obtained by filtration, washed repeatedly with a large amount of water, air dried at room temperature and calcined at 773 K for 6 h to remove the surfactant.

2.1.2. Synthesis of mesoporous aluminosilicates: Al-MCM-41 and Al-SBA-15

For the alumination process, 1.0 g of calcined pure silica (MCM-41 or SBA-15) was added to 50 ml hexane (dry) containing the required amount of aluminium isopropoxide (Si/Al ratio = 5) and stirred at room temperature (*Al-MCM-41*) or 343 K (*Al-SBA-15*) for 24 h. The resulting powders were obtained by filtration, washed with dry hexane, dried at room temperature and calcined at 823 K for 4 h.

2.1.3. Synthesis of phosphoric acid-functionalized MCM-41, SBA-15

Phosphorus species were introduced onto the surface of the calcined silica samples by impregnating 1 g of mesoporous silica (MCM-41 or SBA-15) with 4.5 ml of H_3PO_4 solution (Si/P = 25), according to the method reported by Kawi et al. [27]. In order to prevent the framework from being destroyed in the strong acid solution, the phosphoric acid impregnated samples were rapidly dried under stirring. Finally, the sample was dried in the oven at 373 K for 8 h and calcined at 673 K for 3 h. Samples were designated as MCM-41-P and SBA-15-P.

2.1.4. Synthesis of ethylphophoric acid-functionalized SBA-15

SBA-15-P2: Another phosphoric acid-functionalized SBA-15 sample was prepared by direct synthesis as follows; 4.0 g triblock copolymer poly(ethylene glycol)-blockpoly(propylene glycol)-block-poly(ethylene glycol) ($EO_{20}PO_{20}EO_{20}$) was added to 125 ml of 2 M HCl at room temperature under stirring. Then, the solution was heated to 313 K and 9 g of TEOS was added dropwise. After 45 min, 2.8 g of diethylphosphatoethyltriethoxy silane (DEPTES, Gelest) was added dropwise (to prevent phase separation). The sample was then heated under continuous stirring at 313 K for 2 h by refluxing under microwave heating. The reaction mixture was then transferred to a Teflon-lined autoclave and heated in a conventional oven at 373 K for 24 h. The resulting product was filtered, washed repeatedly with a large amount of water, and dried in air overnight. The surfactant template was removed by extraction with ethanol under reflux for 24 h. Finally, diethylphosphatoethyl groups were cleaved and converted to phosphoric acid groups by refluxing 1 g of diethylphosphatoethyl functionalized SBA-15 in 21 ml of concentrated HCl at 313 K for 24 h.

2.1.5. Synthesis of propylsulfonic acid-functionalized MCM-41

MCM-41-S: A template solution was prepared by dissolving tetramethylammonium hydroxide (TMAOH) and cetyltrimethylammonium bromide (CTAB) in distilled water at 308 K. The silica source, fumed silica, and (3-mercaptopropyl)trimethoxysilane (MPTMS) were then added to the template solution under stirring for 1 h. After further stirring for 1 h the resulting synthesis gel of composition 1 Si: 0.1 MPTMS: 0.25 CTAB: 0.2 TMAOH: 40 H_2O was aged at room temperature for 20 h. Then, the gel was transferred to a Teflon-lined autoclaved and heated at 423 K for 48 h. The solid was recovered by filtration, washed, dried in air at room temperature, and refluxed in ethanol for 24 h. Material with immobilized mercaptopropyl groups was oxidized with H_2O_2 in a methanol–water mixture. Typically, 2.04 g of aqueous 35% H_2O_2 dissolved in three parts of methanol was used per g of material. After 24 h, the suspension was filtered and washed with water and EtOH. The wet material was resuspended (1 wt%) in acidified H_2O (0.1 M H_2SO_4) for another 4 h. Finally, the solid was extensively rinsed with H_2O, dried at 333 K, and stored in a desiccator.

2.1.6. Synthesis of arenesulfonic acid-functionalized HMS

HMS was synthesized at 338 K from a gel containing 0.02 TEOS, 0.005 amine, 0.088 EtOH and 2.56 H_2O. The amine (dodecylamine (dda), hexadecylamine (hda) or octadecylamine (oda)) was first dissolved in an alcohol–water mixture. TEOS was then added and the mixture was stirred at 338 K for 24 h. The amine template was removed by calcining at 873 K for 4 h to generate HMS samples designated as HMS(dda), HMS(hda) and HMS(oda) for templating via dodecylamine (dda), hexadecylamine (hda) or octadecylamine (oda), respectively. Then, the HMS samples were treated with 1.5 g of (2-(4-chlorosulfonylphenyl)ethyltriethoxysilane (CSPTMS) by refluxing at 313 K for 2 h to introduce the organosulfonic groups.

Sulfonated samples were designated as HMS(dda)-S, HMS(hda)-S and HMS(oda)-S.

2.2. Catalysts characterization

Powder X-ray diffraction (XRD) patterns were performed using a Bruker AXS D8 Advance powder diffractometer with Cu $K\alpha$ radiation (40 kV, 40 mA), a 0.020° step size, and a 1 s step.

Elemental composition (Si/Al ratio) was determined with a Philips MiniPal PW4025 X-ray fluorescence (XRF) instrument and an average taken over three runs.

Textural properties were determined via nitrogen sorption analysis at 77 K using a conventional volumetric technique by a Micromeritics ASAP 2020. Before analysis the samples were oven-dried at 423 K and evacuated overnight at 423 K under vacuum. The surface area was calculated using the standard Brunauer–Emmett–Teller (BET) method using adsorption data in the relative pressure range from 0.05 to 0.2. The total pore volume was estimated on the basis of the amount of nitrogen adsorbed at a relative pressure (P/P_o) of ca. 0.99.

The acid content of aluminosilicates was determined using established procedures that employ thermal desorption of cyclohexylamine (CHA) [31]. The mass loss associated with desorption of the base from acid sites was used to calculate the total acid content (mmol of CHA/g of sample) assuming that each acid site interacts with one base molecule. To obtain the content of strong acid sites, the CHA-containing samples dried at 353 K were further heated in an oven at 523 K prior to TGA analysis.

The acid capacity of sulfonated samples was measured through the determination of cation-exchange capacities using aqueous sodium chloride (2 M) solutions as cationic-exchange agent. Released protons were then potentiometrically titrated [32].

Thermogravimetric analysis (TGA) technique was used to confirm and quantify the introduction of the sulfonic acid groups (sulphur content) for all sulfonic acid-functionalized samples and the amount of phosphoric groups (phosphorous content) in sample SBA-15-P2 since the weight loss observed between 360 °C and 660 °C in the TGA has been related in the literature to the loss of the incorporated organic acid groups [28,32]. Thermogravimetric analyses were performed in a TA instruments equipment from 50 °C to 800 °C at 10 °C/min under airflow.

Scanning electron microscopy (SEM) were performed on a scanning electron microscope, JEOL JSM6400, operating at accelerating voltage of 25 kV and work distances of 10 mm, and magnification of 10,000×.

2.3. Catalytic activity

Etherification experiments were performed in the liquid phase in a stainless steel stirred autoclave (150 mL) equipped with temperature controller and a pressure gauge. Stirring was fixed for all experiments at 1200 rpm to avoid external diffusion limitations. Liquid phase pressurized isobutene (glycerol/isobutene molar ratio of 0.25) was injected into the reactor, previously charged with glycerol and catalyst (0.5 g), using nitrogen at 10 bar as pushing agent. The temperature was then raised to 348 K and the pressure increased accordingly following the liquid–vapour equilibrium. Catalytic experiments were made at 24 h. The reaction products were analyzed by gas chromatography using a chromatograph model Shimadzu GC-2010 equipped with a SupraWax-280 column and a FID detector. Glycerol conversion and selectivity to MTBG (glycerol monoethers) were determined from calibration lines obtained from commercial products. For DTBG (glycerol diethers) and TTBG (glycerol triether), which were not available commercially, we isolated them from the products of the etherification reaction by column chromatography (1:9 ethyl acetate/hexane) and identified them by ^{13}C and ^{1}H NMR for proper quantification [16] with the assistance of the characterization data reported by Jamróz et al. [33].

3. Results and discussion

3.1. Catalysts characterization

XRD patterns of synthesized and modified MCM-41 and SBA-15 samples were typical of well-ordered hexagonal materials whereas HMS samples showed only one peak typical of a wormhole type pore structure (Fig. 1). The structure of mesoporous silicas was generally well maintained after Al insertion, or after incorporation of phosphoric or sulfonic groups. Some decrease of ordering was, however, apparent for organosulfonic acid functionalized samples for which a relatively greater loss in long-rangemesostructural ordering was observed (Fig. 1).

Si/Al ratios of aluminosilicates (Al-MCM-41 and Al-SBA-15) were slightly higher (7.3 and 7.8, respectively) than the theoretical gel ratios (Si/Al = 5). Both aluminated samples retained good mesostructural ordering and narrow pore size distribution, as deduced from the nitrogen sorption isotherms and pore size distribution curves shown in Figs. 2 and 3. The aluminated samples had lower surface area and pore volumes than their corresponding pure silicas (Table 1). The thicker pore walls of the Al-grafted materials, coupled with the presence of non-framework Al in the pores may be responsible for this decrease. The introduction of aluminium in the structure increased the acidity of the materials (Table 1), as expected. The differences in acidity observed between the two aluminosilicates can be related to their different Si/Al ratio.

XRD and N_2 sorption analysis results of the phosphoric acid-functionalized samples (MCM-41-P, SBA-15-P, SBA-15-P2) showed that the structure and uniform framework could still be well maintained after external introduction of phosphorous species onto the pore surface via post-synthesis impregnation in phosphoric acid solution or direct synthesis (Figs. 1–3). Therefore, the incorporation of phosphorus species under the conditions used did not degrade the mesoporous structure of the materials. However, we observed a decrease in the surface area and pore volume (Table 1), which can be attributed to the presence of phosphoric groups in the pores. The phosphorous content was higher for the sample prepared by direct synthesis (Si/P = 15.6), as determined from TGA, than for the samples in which phosphoric acid groups were introduced by post-synthesis impregnation (Si/P = 25).

Finally, after sulfonation, a significant decrease in surface area, pore volume and average pore size was obtained for all samples (Table 1). This is as expected since sulfonic acid groups extend into the pores, reducing pore diameter and volume. However, the uniform silica framework was maintained, as indicated by the nitrogen sorption isotherms and pore size distribution curves shown in Figs. 4 and 5. The higher decrease of surface area observed for sample HMS(dda)-S, which was synthesized using dodecylamine as surfactant, with respect to the other sulfonated HMS samples could be attributed to a higher content of sulfonic groups. Interestingly, HMS(dda)-S exhibited additional capillary condensation at partial pressures > 0.90 due to the filling of textural mesopores (Fig. 4), which was not observed for the other HMS samples synthesized with surfactants of higher carbon chain length. The degree of textural porosity in HMS depends both on the nature of the surfactant and the solvent polarity used during the synthesis, as previously reported [30,34]. The textural mesopores are important because they greatly facilitate mass transport to the framework mesopores [29,30].

Fig. 6 shows the particle morphology of sulfonated HMS samples. Sulfonated HMS synthesized with dodecylamine exhibited

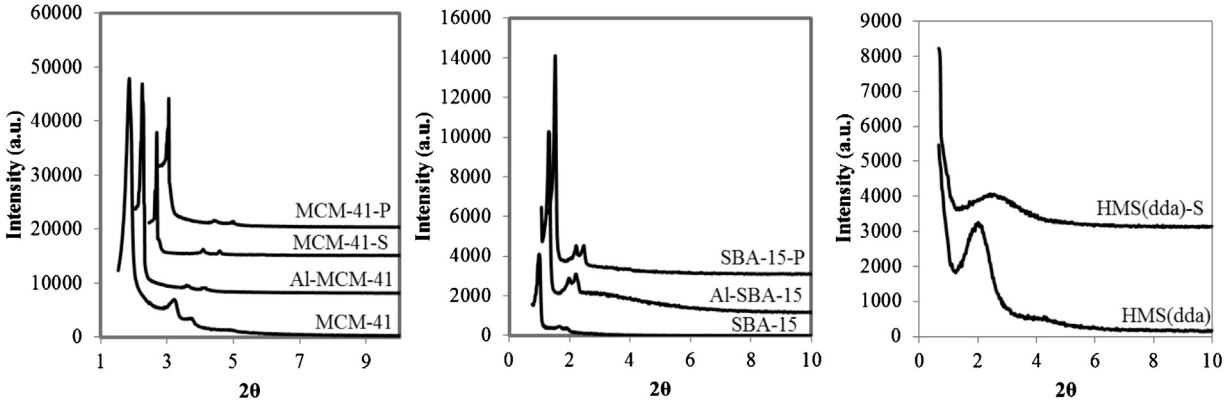

Fig. 1. XRD patterns of several MCM-41, SBA-15 and HMS samples.

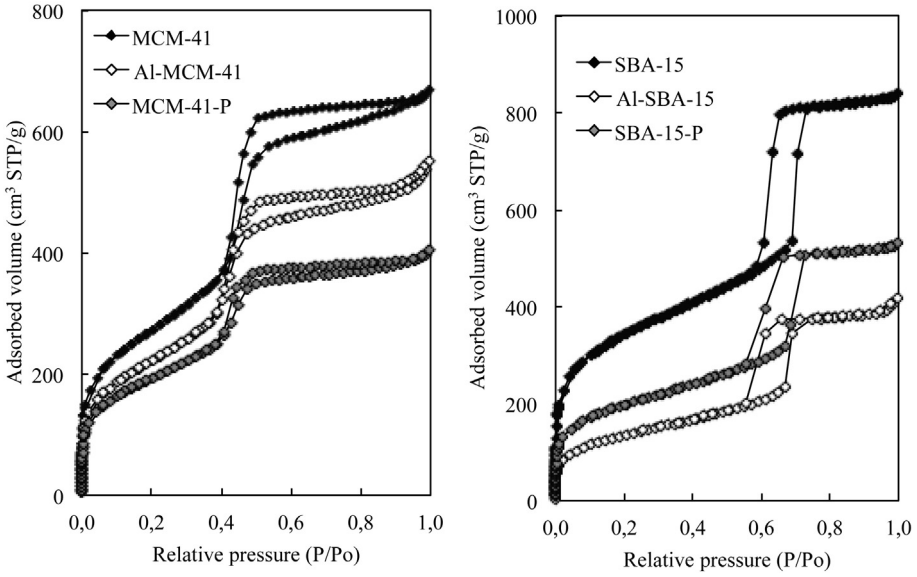

Fig. 2. Nitrogen adsorption-desorption isotherms of MCM-41, Al-MCM-41, MCM-41-P, SBA-15, Al-SBA-15 and SBA-15-P.

Table 1
Textural properties, acidity and sulfur content of the materials.

Catalyst	Surface area (m^2/g)	Average pore diameter (nm)	Total pore volume (cm^3/g)	Acid capacity(meq H^+/g)[a]	Sulfur content[b]
MCM-41	989	3.93	1.04	–	–
SBA-15	1212	7.31	1.30	–	–
HMS(dda)	612	4.03	1.96	–	–
HMS(hda)	703	4.07	1.27	–	–
HMS(oda)	632	4.79	1.30	–	–
Al-MCM-41	808	3.63	0.86	0.81	–
Al-SBA-15	488	6.92	0.65	0.55	–
MCM-41-P	696	3.80	0.63	–	–
SBA-15-P	704	7.57	0.82	–	–
SBA-15-P2	643	7.85	0.71	–	–
MCM-41-S	807	3.37	1.29	0.24	0.20
HMS(dda)-S	497	4.01	1.65	0.63	0.64
HMS(hda)-S	693	4.06	1.10	0.15	0.13
HMS(oda)-S	628	4.81	1.15	0.10	0.08

[a] Determined by thermal desorption of cyclohexylamine for Al-containing samples and by potentiometric titration for sulfonated samples.
[b] (mmol organic sulfonic acid group per g sample) calculated from TGA.

smaller particle sizes than sulfonated HMS synthesized with hexadecylamine or octadecylamine. These small particles (<200 nm) are consistent with the complementary textural mesoporosity observed from N_2 sorption data.

TGA confirmed that all sulfonated samples possessed sulfonic groups since a weight loss between 360 °C and 660 °C was observed (Fig. 7). This weight loss has been related to the loss of organic sulfonic groups [16–18,32,35], and allowed us to calculate the sulfur content as mmol organic sulfonic group/g sample (Table 1). It is important to note that for sulfonated HMS samples, HMS(dda)-S showed much higher sulfur content than HMS(hda)-S and HMS(oda)-S (Table 1, Fig. 7). This confirms a higher incorporation

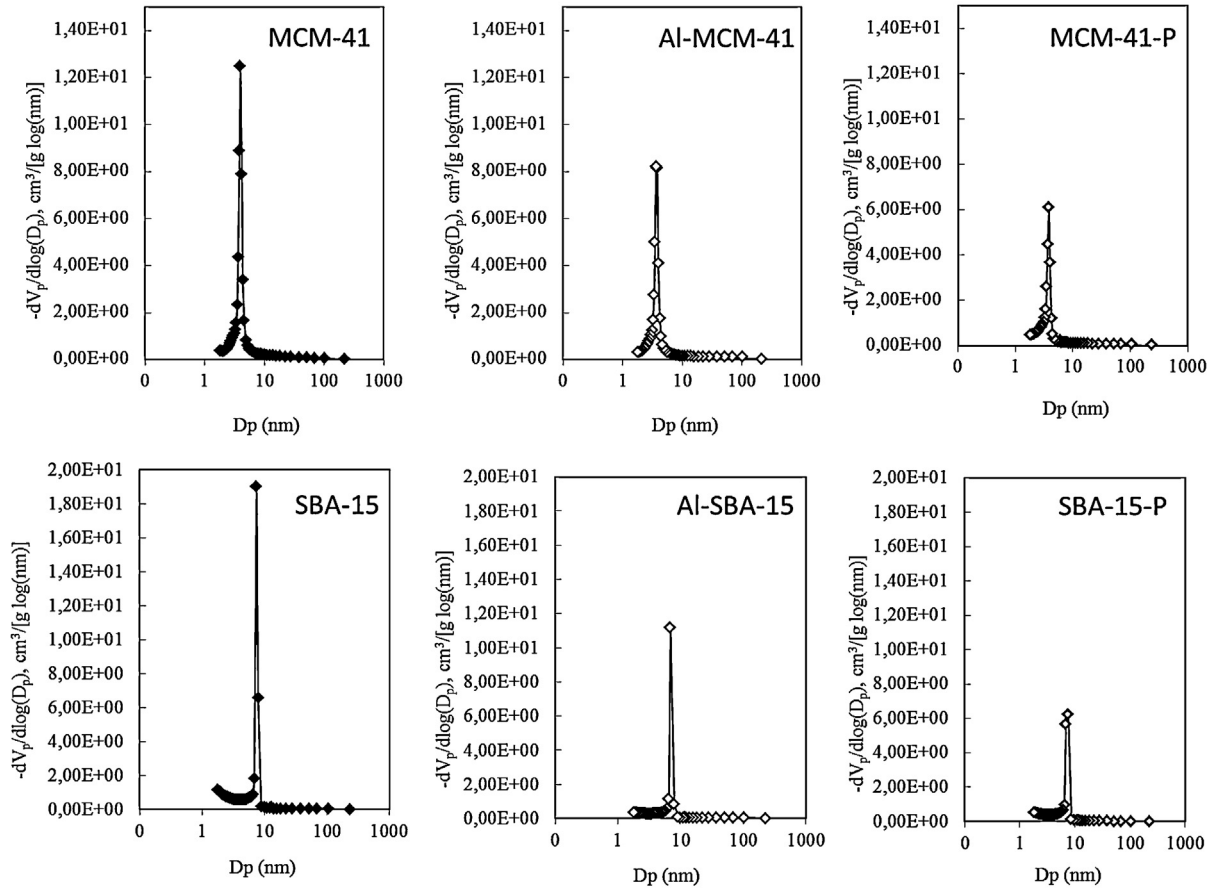

Fig. 3. Pore size distribution graphics of MCM-41, Al-MCM-41, MCM-41-P, SBA-15, Al-SBA-15 and SBA-15-P.

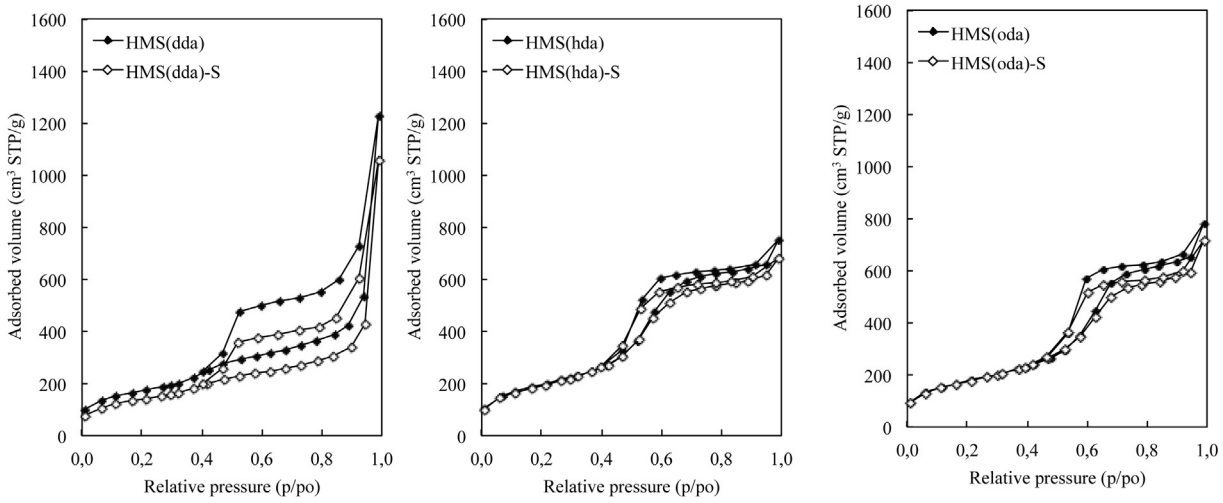

Fig. 4. Nitrogen adsorption-desorption isotherms of HMS(dda), HMS(dda)-S, HMS(hda), HMS(hda)-S, HMS(oda) and HMS(oda)-S.

of sulphonic groups in HMS(dda)-S. The acidity of sulfonated samples, determined potentiometrically, was higher for the samples that showed higher amounts of sulfonic groups, in agreement with TGA results (Table 1).

3.2. Catalytic activity

Initially, several tests were performed at low reaction time (4 h). The results showed low conversion and high selectivity to MTBG, without detection of TTBG for all catalysts except for catalyst HMS(dda)-S, which had moderate conversion and yielded moderate amounts of DTBG and low amounts of TTBG. Thus, we decided to test the catalysts at longer reaction time in order to try to obtain higher amounts of h-GTBE.

Table 2 and Fig. 8 show the catalytic activity results of pure silicas and modified MCM-41, SBA-15 and HMS catalysts, respectively, for the etherification reaction of glycerol with isobutene after 24 h of reaction. The reaction products were mono-*tert*-butyl glycerol

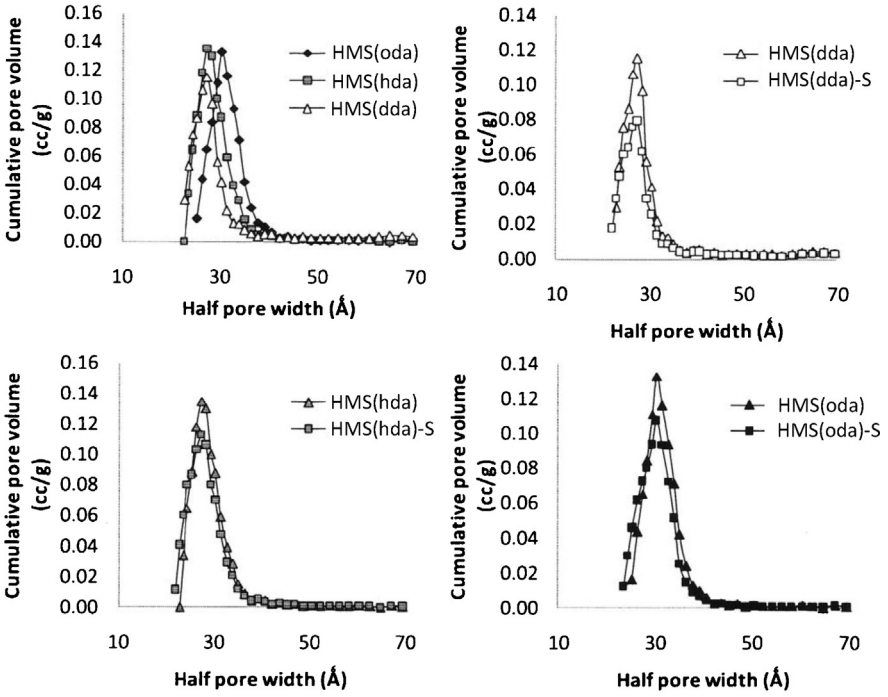

Fig. 5. Pore size distribution graphics of HMS(dda), HMS(dda)-S, HMS(hda), HMS(hda)-S, HMS(oda) and HMS(oda)-S.

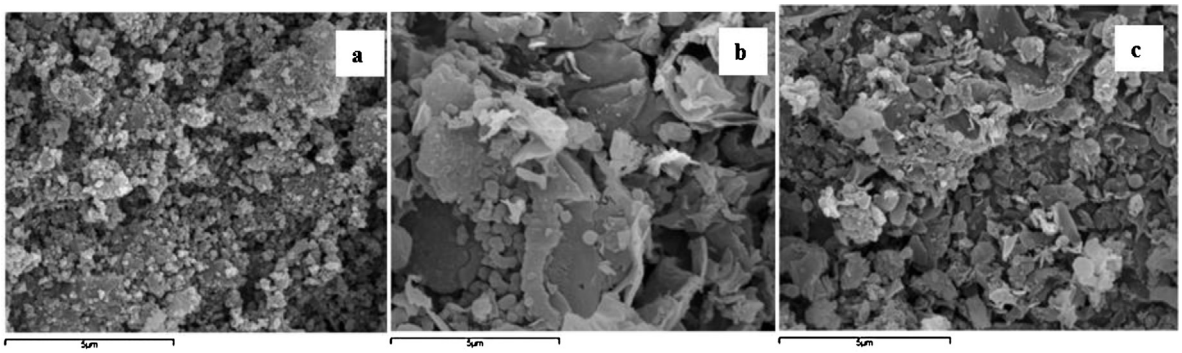

Fig. 6. Scanning electron micrographs of samples: (a) HMS(dda)-S, (b) HMS(hda)-S and (c) HMS(oda)-S.

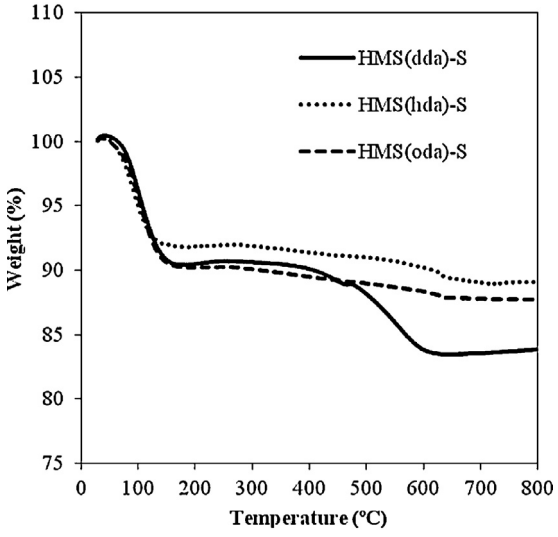

Fig. 7. TGA curves of HMS(dda)-S, HMS(hda)-S and HMS(oda)-S.

Table 2
Catalytic activity of pure silica samples.

Catalyst	Conversion (%)	Selectivity to MTBG (%)	Selectivity to h-GTBE (%)[a]
MCM-41	20	87	13
SBA-15	23	89	11
HMS(dda)	30	88	12
HMS(hda)	25	93	7
HMS(oda)	23	95	5

MTBG: glycerol monoethers.
[a] Selectivity to glycerol diethers since glycerol triether was not detected.

ether (MTBG), di-*tert*-butyl glycerol ether (DTBG) and tri-*tert*-butyl glycerol ether (TTBG). Additionally, diisobutylene was detected in very low amounts for all samples.

Pure silica (MCM-41 SBA-15, HMS) showed the lowest conversion and lowest selectivity to h-GTBE due to their low content of acid sites (Table 2). The incorporation of aluminium in the structure of MCM-41 and SBA-15 increased the amount of Brønsted acid sites, leading to higher conversion values than the corresponding pure silicas, but their low acid strength resulted in low selectivity to h-GTBE with glycerol triether not being detected. In previous work,

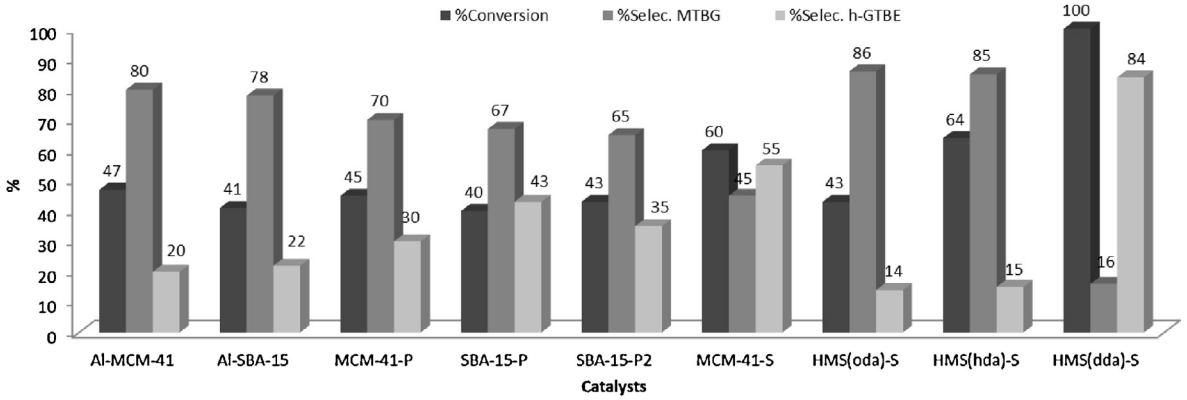

Fig. 8. Catalytic activity of modified MCM-41, SBA-15 and HMS for the glycerol etherification after 24 h.

we concluded that the acidity strength influences significantly the catalytic performance, especially the selectivity to h-GTBE [15–18].

The incorporation of phosphoric groups (MCM-41-P, SBA-15-P and SBA-15-P2) also led to moderate conversion values (40–45%) but higher selectivity to h-GTBE was obtained (30–43%) (Fig. 8) and tri-*tert*-butyl ether of glycerol was detected in low amounts (2–8%). The higher acid strength of phosphoric groups can explain these results. Although catalyst SBA-15-P2 had higher amount of incorporated phosphoric acid groups, its catalytic results were similar to those obtained with the silicas impregnated with phosphoric acid. This means that some phosphoric groups in SBA-15-P2 were not accessible to the reactants.

For sulfonic acid-functionalized samples, by increasing the amount of sulfonic groups, higher conversion was obtained. Sulfonic acid-functionalized MCM-41 led to higher conversion and higher selectivity to h-GTBE than Al-MCM-41 and MCM-41-P. This confirms the significant role of the strength of Brønsted acid sites. It is well know that the Brønsted acid strength is influenced by the nature of the acid group (e.g., $-SO_3H > -COOH$), the electronic properties of the organic backbone, the surface concentration of the acid moieties, and the solvent used [36,37]. A direct approach for the determination of the acid strength is the measurement of the p*K*a value of the organic-inorganic material. Mauder et al. [38] determined that sulfonic acid-functionalized SBA-15 and phosphonic acid-functionalized SBA-15 exhibited p*K*a values of about 0.6 and 1.3, respectively whereas pure silica SBA-15 showed p*K*a value around 5. McKeen et al. also reported that sulfonic acid containing samples had higher proton conductivities than phosphoric acid functionalized materials [28].

Interestingly, HMS(dda)-S exhibited total conversion and 84% selectivity to h-GTBE (with 26% to glycerol triether) after 24 h of reaction (Fig. 7). These results are better than those obtained with a commercial Amberlyst-15 catalyst, a macroporous strong acid ion-exchange resin, which showed 99% of conversion and 77% selectivity to h-GTBE (with 19% to glycerol triether) under similar reaction conditions [16]. The differences observed in the activity between the three sulfonated HMS could be explained by the different amount of incorporated sulfonic acid groups. The generation of textural porosity in the HMS synthesized with dodecylamine favoured the introduction of higher amounts of sulfonic groups and their accessibility, which explains the observed results.

All sulfonated HMS catalysts maintained their sulfur content after reaction, as determined by TGA. This confirms that there was no leaching of the sulfonic acid groups during reaction. However, from N_2 sorption data, we observed a decrease of surface area after reaction, although this decrease was much lower for catalyst HMS(dda)-S (Fig. 9). The decrease of surface area observed after reaction can be explained by the presence of reagents and

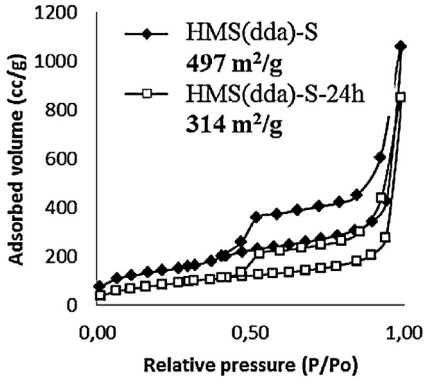

Fig. 9. Nitrogen adsorption–desorption isotherms of HMS(dda)-S and HMS(dda)-S-24 h (after reaction).

reaction products in the pores, as previously observed for other microporous/mesoporous catalysts for this reaction [16,18]. Therefore, the additional textural porosity of HMS(dda)-S affords greater resistance to deactivation of the catalyst.

4. Conclusions

The incorporation of aluminium in the structure of MCM-41 and SBA-15 increased the amount of Brønsted acid sites, leading to higher conversion for glycerol etherification with isobutene than pure silicas, but their weak acid strength resulted in low selectivity to h-GTBE. The incorporation of phosphoric groups allows us to detect the tri-*tert* butyl ether of glycerol in low amounts. However, the strength of phosphoric groups was not enough to obtain high selectivity to di- and tri-ethers (h-GTBE). On the other hand, sample HMS(dda)-S, which showed textural mesoporosity, exhibited total conversion and 84% selectivity to h-GTBE (26% to triether) after 24 h of reaction.

The degree of complementary textural porosity in mesoporous silica HMS depends on the surfactant used during the synthesis. The generation of textural mesoporosity reduced diffusion limitations, and consequently increased the incorporation of sulfonic groups into HMS and their accessibility, leading to higher catalytic activity.

Acknowledgments

The authors are grateful for the financial support of the Ministerio de Economía y Competitividad and FEDER funds (CTQ2008-04433 and (CTQ2011-24610).

References

[1] R.S. Karinen, A.O.I. Krause, Appl. Catal., A 306 (2006) 128–133.
[2] K. Klepáčová, D. Mravec, E. Hájeková, M. Bajus, Pet. Coal 45 (2003) 54–57.
[3] K. Klepáčová, D. Mravec, M. Bajus, Appl. Catal., A 294 (2005) 141–147.
[4] K. Klepáčová, D. Mravec, A. Kaszony, M. Bajus, Appl. Catal., A 328 (2007) 1–13.
[5] J.A. Melero, G. Vicente, G. Morales, M. Paniagua, J.M. Moreno, R. Roldán, A. Ezquerro, C. Pérez, Appl. Catal., A 346 (2008) 44–51.
[6] J.A. Melero, J. Iglesias, G. Morales, Green Chem. 11 (2009) 1285–1308.
[7] M. Di Serio, L. Casale, R. Tesser, E. Santacesaria, Energy Fuels 24 (2010) 4668–4672.
[8] H.J. Lee, D. Seung, K.S. Jung, H. Kim, I.N. Filimonov, Appl. Catal., A 390 (2010) 235–244.
[9] L. Xiao, J. Mao, J. Zhou, X. Guo, S. Zhang, Appl. Catal., A 393 (2011) 88–95.
[10] W. Zhao, B. Yang, C. Yi, Z. Lei, J. Xu, Ind. Eng. Chem. Res. 49 (2010) 12399–12404.
[11] P.M. Slomkiewicz, Appl. Catal., A 313 (2006) 74–85.
[12] R. Luque, V. Budarin, J.H. Clark, D. Macquarrie, Appl. Catal., B 82 (2008) 157–162.
[13] F. Frusteri, F. Arena, G. Bonura, C. Cannilla, L. Spadaro, O. Di Blasi, Appl. Catal., A 367 (2009) 77–83.
[14] N. Ozbay, N. Oktar, N.A. Tapan, Int. J. Chem. Reactor Eng. 8 (A18) (2010) 1–10.
[15] M.D. González, Y. Cesteros, P. Salagre, Appl. Catal., A 450 (2013) 178–188.
[16] M.D. González, Y. Cesteros, P. Salagre, J. Llorca, J. Catal. 290 (2012) 202–209.
[17] M.D. González, P. Salagre, E. Taboada, J. Llorca, E. Molins, Y. Cesteros, Appl. Catal., B 136–137 (2013) 287–293.
[18] M.D. González, P. Salagre, E. Taboada, J. Llorca, Y. Cesteros, Green Chem. (2013).
[19] F. Frusteri, L. Frusteri, C. Cannilla, G. Bonura, Bioresour. Technol. 118 (2012) 350.
[20] A. Behr, J. Eilting, K. Irawadi, J. Leschinski, F. Lindner, Green Chem. 10 (2008) 13–30.
[21] A.C. Carmo Jr., L.K.C. de Souza, C.E.F. da Costa, E. Longo, J.R. Zamian, G.N. da Rocha Filho, Fuel 88 (2009) 461–468.
[22] A. Ungureanu, B. Dragoi, V. Hulea, T. Cacciaguerra, D. Meloni, V. Solinas, E. Dumitriu, Microporous Mesoporous Mater. 163 (2012) 51–64.
[23] R. Mokaya, J. Phys. Chem. B 104 (2000) 8279–8286.
[24] Y. Yue, A. Gédéon, J.L. Bonardet, N. Melosh, J.B. D'Espinose, J. Fraissard, Chem. Commun (1999) 1967–1968.
[25] R. Mokaya, Chem. Phys. Chem. 4 (2002) 360–363.
[26] J. Połtowicz, K. Pamin, L. Matachowski, E.M. Serwicka, R. Mokaya, Y. Xia, Z. Olejniczak, Catal. Today 114 (2006) 287–292.
[27] S. Kawi, S.C. Shen, P.L. Chew, J. Mater. Chem. 12 (2002) 1582–1586.
[28] J.C. McKeen, Y.S. Yan, M.E. Davis, Chem. Mater. 20 (2008) 5122–5124.
[29] T.R. Pauly, Y. Liu, T.J. Pinnavaia, S.J.L. Billinge, T.P. Rieker, J. Am. Chem. Soc. 121 (1999) 8835–8842.
[30] W. Zhang, T.R. Pauly, T.J. Pinnavaia, Chem. Mater. 9 (1997) 2491–2498.
[31] R. Mokaya, W. Jones, S. Moreno, G. Poncelet, Catal. Lett. 49 (1997) 87–94.
[32] J.A. Melero, G.D. Stucky, R. van Grieken, G. Morales, J. Mater. Chem. 12 (2002) 1664–1670.
[33] M.E. Jamróz, M. Jarosz, J. Witowska-Jarosz, E. Bednarek, W. Tecza, M.H. Jamróz, J.C. Dobrowolski, J. Kijenski, Spectrochim. Acta, Part A 67 (2007) 980–988.
[34] F. Di Renzo, F. Testa, J.D. Chen, H. Cambon, A. Galarneau, D. Plee, F. Fajula, Microporous Mesoporous Mater. 28 (1999) 437–446.
[35] D. Margolese, J.A. Melero, S.C. Christiansen, B.F. Chmelka, G.D. Stucky, Chem. Mater. 12 (2000) 2448.
[36] I.K. Mbaraka, B.H. Shanks, J. Catal. 244 (2006) 78.
[37] D. Fărcaşiu, A. Ghenciu, G. Marino, K.D. Rose, J. Am. Chem. Soc. 119 (1997) 11826.
[38] D. Mauder, D. Akcakayiran, S.B. Lesnichin, G.H. Findenegg, I.G. Shenderovich, J. Phys. Chem. C. 113 (2009) 19185.